

# Microstructure and abrasive wear behaviour of $B_4C$ particle reinforced 2014 Al matrix composites

A. Canakci

Received: 17 August 2010/Accepted: 4 December 2010/Published online: 16 December 2010  
© Springer Science+Business Media, LLC 2010

**Abstract** In this study, the microstructure and abrasive wear properties of varying volume fraction of particles up to 12%  $B_4C$  particle reinforced 2014 aluminium alloy metal matrix composites produced by stircasting method was investigated. The density, porosity and hardness of composites were also examined. Wear behaviour of  $B_4C$  particle reinforced aluminium alloy composites was investigated by a block-on-disc abrasion test apparatus where the samples slid against the abrasive suspension mixture (contained 10 vol.% SiC particles and 90 vol.% oil) at room conditions. Wear tests performed under 92 N against the abrasive suspension mixture with a novel three body abrasive. For wear behaviour, the volume loss and specific rate of the samples have been measured and the effects of sliding time and the content of  $B_4C$  particles on the abrasive wear properties of the composites have been evaluated. The dominant wear mechanisms were identified using SEM. Microscopic observation of the microstructures revealed that dispersion of  $B_4C$  particles was generally uniform while increasing volume fraction led to agglomeration of the particles and porosity. The density of the composite decreased with increasing reinforcement volume fraction but the porosity and hardness increased with increasing particle content. Moreover, the specific wear rate of composite decreased with increasing particle volume fraction. The wear resistance of the composite was found to be considerably higher than that of the matrix alloy and increased with increasing particle content.

## Introduction

Metal matrix composites (MMCs) are being increasingly used in the aerospace and automobile industries because of their improved strength, stiffness and increased wear resistance over unreinforced alloys [1–5]. The commonly used metallic matrices include light metals such as aluminium, magnesium, titanium and their alloys. The reinforcement can be in the form of fibres, whiskers and particulates [4, 5]. Aluminium (Al)-based MMCs have a very low coefficient of thermal expansion and high specific strengths, wear resistance and heat resistance as compared to the conventional Al alloys [6–8]. Al-MMCs can substitute for steel to some degree when reinforced with ceramic particulate materials such as SiC,  $Al_2O_3$ ,  $B_4C$ , TiC [9, 10]. Consequently, they have a great potential of application in defense and automotive industries [11–14].

A number of particulate composites have been produced, either by adding particles externally [15, 16] or by manipulating solidification as in rheocasting [17], to result in spherical primary particles embedded in a matrix. Most of the fabrication methods have employed stirring to create a vortex. The negative pressure differential existing at the vortex helps to suck externally added particles into the liquid metal. However, the vortex also sucks in air bubbles in the particle-melt slurry, resulting in large porosities in the cast composites [18]. Broadly, there are two types of foundry methods for producing composites with externally added particles, depending on the temperature at which the particles are introduced into the melt. In the liquid metallurgy process [15], the particles are added above the liquid temperature of the molten alloy whereas in compo-casting the particles are introduced into the semi-solid slurry temperature range. In both of these processes the vortex is used and the composites have high porosity [18].

A. Canakci (✉)  
Department of Metallurgical and Materials Engineering,  
Karadeniz Technical University, 61080 Trabzon, Turkey  
e-mail: aykut@ktu.edu.tr

Wear behaviour in MMCs can be divided into two categories depending upon the nature of reinforcements. These are metal/alloys containing: soft reinforcements like graphite [19] or hard particles like SiC, Al<sub>2</sub>O<sub>3</sub>, TiO<sub>2</sub> [20], etc. The presence of hard particles into the matrix also influences its wear behaviour. The use of hard ceramic particles like Al<sub>2</sub>O<sub>3</sub>, SiC, as reinforcements in the metallic matrix have shown to reduce the wear loss more as compared to the base alloys [21]. In general, it has been observed [21–23] that the wear rate decreases both by increasing the volume fraction of hard phase and the particles size. Further, the use of hard phase helps in pushing the seizure on the higher load at constant sliding velocity.

The abrasive wear depends on various factors like abrasive size [24–30], rake angle of abrasives [24, 31, 32], applied load [21, 24, 29, 33] and shape, size and volume fraction of the dispersoid phases [34–36]. In addition to these factors the abrasive wear rate of a material also depends on the surface hardness [29, 31, 33, 37] and materials properties like fracture toughness [31, 33, 38–40].

The aim of the present study, therefore, was to: (a) investigate the effect of B<sub>4</sub>C particles content on the microstructure and porosity; (b) research the abrasive wear behaviour of aluminium alloy and its composite under three-body abrasive wear testing condition; (c) examine the effect of B<sub>4</sub>C particles content and sliding time on the abrasive wear behaviour of composites as compared to that of the matrix alloy.

## Experimental procedure

In this study, AA2014 alloy with the theoretical density of 2.78 g/cm<sup>3</sup> was used as the matrix material while B<sub>4</sub>C particles with average particle size of 85 µm which varies between 45 µm and 125 µm and a density of 2.52 g/cm<sup>3</sup> were used as the reinforcements. The AA2014 alloy was supplied by Seydişehir Aluminium Co located in Konya, Turkey. The chemical composition (in wt%) of the AA2014 alloy was as follows: 0.955% Si, 0.269% Fe, 5.570% Cu, 0.656% Mn, 0.742% Mg, 0.006% Zn, 0.019% Ti, 0.002% Cr, with the balance being Al. The B<sub>4</sub>C particles were supplied from Wacker Ceramics Kempton GmbH (Kempten, Germany) and the chemical composition was given in Table 1 [41].

**Table 1** The chemical composition of B<sub>4</sub>C particles (in wt%)

Particles	B	C	B <sub>2</sub> O <sub>3</sub>	Fe	O	N	Si
Macrogrits (F10-F220)	min. 76	min. 19.5	max. 0.5	max. 0.15	max. 1.0	max. 1.0	max. 0.15

All samples used in this investigation were produced by stircasting technique. Details of the experimental set-up and production processes are reported in the previous study [42]. Unreinforced 2014 Al matrix alloy sample was also produced by the same method.

The experimental density of the composite samples was measured using Archimede's method. In this technique, density is determined by measuring the difference between the sample's weight in air and when it was suspended in distilled water at room temperature. The theoretical density was calculated using the mixture rule according to the the volume fraction of the B<sub>4</sub>C particles. The porosities of the composites were then evaluated from the difference between the expected and the observed density of each sample.

The hardness of the samples was measured using Brinell hardness method under a load of 31.25 kg.

The microstructures of the produced ingots were examined using a SEM to determine the distribution of the B<sub>4</sub>C particles in the matrix and presence of porosity. For this purpose, the samples were first sectioned and then prepared following the standard metallographic technique.

The three body wear tests were carried out on B<sub>4</sub>C particles reinforced composites and matrix alloy samples using a block-on-disc machine (Plint & Partners Wear Tester) at ambient temperature in the laboratory conditions. The Wear tester was modified for the three body wear tests, as shown in Fig. 1. The apparatus consists of an electric motor of 3 kW power, a data collector controller, a disc, a sample holder, a supporter handle, and a pipe system giving the abrasive suspension mixture between sample (block) and disc. The test samples were slid against a disc (counterface) having the diameter of 60 mm and length of 12 mm. The disc material was 4140 grade steel with a hardness of 60 HRC. The test samples were cut from the composite ingot as shown in Fig. 2.

Wear tests were carried out under normal load of 92 N and with total sliding time of 2080 s. The samples were tested in five sliding times: 200, 670, 1140, 1610 and 2080 s. The weight loss during the sliding tests were calculated using weight differences of samples before and after tests to the nearest 0.1 mg. The wear test was interrupted at regular intervals and the weight loss of the sample was recorded. After each weight loss (and before weighing) the sample and disc were first cleaned in an ultrasonic bath with acetone and then dried below 100 °C. The weight loss was converted into volume loss using the density of the

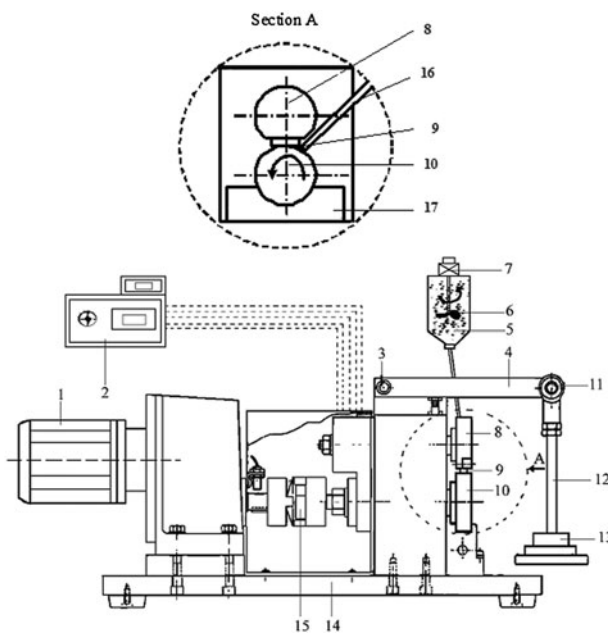


**Fig. 1** Schematic diagram of the abrasion wear test apparatus for the three body wear tests. (1) Electric motor, (2) data collector controller, (3) pin, (4) loading rod, (5) the abrasive suspension mixture, (6) stirrer motor, (7) stirrer motor, (8) sample holder, (9) sample, (10) disc, (11) swivel joint, (12) supporter handle, (13) weight, (14) bottom table, (15) clutch, (16) pipe system giving the abrasive suspension mixture between sample and disc, (17) concentration container of the abrasive suspension mixture

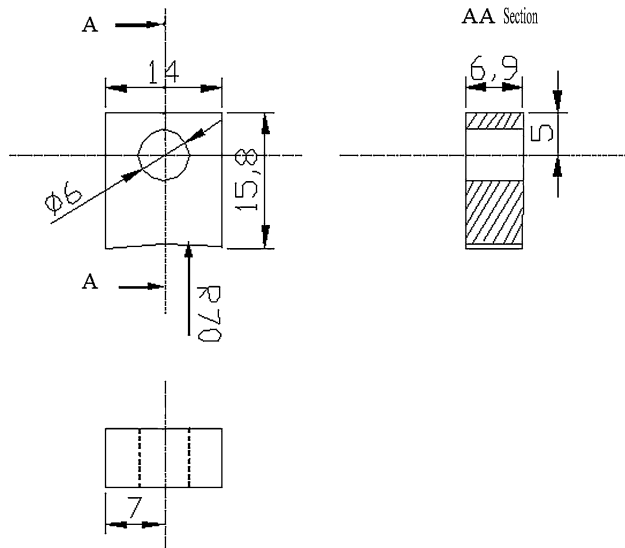


**Fig. 2** The wear test sample

samples. For each test condition, at least three tests were performed and the average of them was used. The tests were conducted at a rotational speed of 100 rpm (corresponding to a linear velocity of  $0.314 \text{ m s}^{-1}$ ). The abrasive suspension mixture used was fresh whereas the sample remained unchanged throughout the entire range of sliding

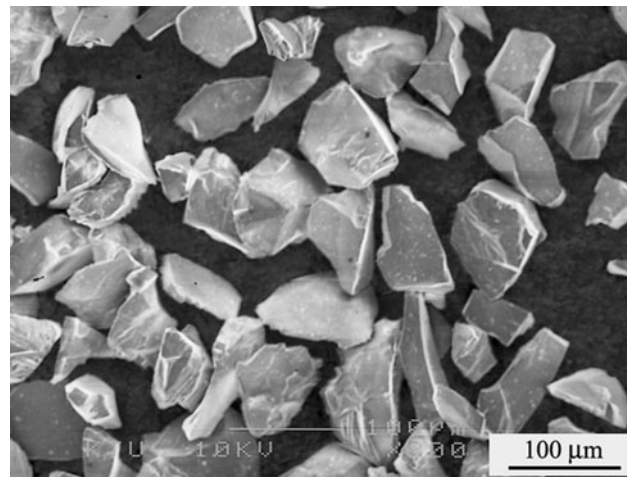


**Fig. 3** Scanning electron micrographs of SiC abrasive particles

times. The abrasive suspension mixture containing 10 vol.% SiC particles and 90 vol.% oil was used as abrasion. The size of SiC particles range from 63 to 125  $\mu\text{m}$  (average particle size 90  $\mu\text{m}$ ) were separately used for conducting the abrasion tests. The feeding rate of the abrasive suspension mixture was about  $0.37 \text{ mL s}^{-1}$ . The morphological feature of the SiC particles is shown Fig. 3, where the particles are generally angular in shape with sharp edges.

After wear tests, the specific wear rates were calculated using the equation [43] given below:

$$W = \frac{\Delta m}{\rho \cdot F_n \cdot v \cdot t} = \frac{V}{F_n \cdot v \cdot t} \quad (1)$$

where  $W$  ( $\text{mm}^3/\text{Nm}$ ),  $\Delta m$  (g),  $\rho$  ( $\text{g/mm}^3$ ),  $V$  ( $\text{mm}^3$ ),  $F_n$  (N),  $v$  ( $\text{m/s}$ ), and  $t$  (s) are the specific wear rate, the mass loss, the density, the volume loss, the normal load, the sliding velocity and the sliding time, respectively.

The worn surfaces of samples subjected to both abrasive and sliding wear tests were examined using the SEM.

The roughness of the composite surfaces was evaluated by surface texture measurements using a stylus-type instrument. The surface texture parameter  $R_a$  ( $\mu\text{m}$ ) was used to indicate the surface roughness after each of the abrasive wear tests. The surface roughness values were measured before and after the sliding tests. Before the wear tests, each sample surface was ground with a 800 grade abrasive paper for being comparison of surface roughness of each sample.

## Results and discussion

The compositions and properties of the AA2014 alloy and its composite reinforced with  $B_4C$  particles are given in Table 2.

**Table 2** Material properties of the Al alloy and reinforced-composite samples

Code	Composition	Theoretical density ( $\text{g cm}^{-3}$ )	Experimental density ( $\text{g cm}^{-3}$ )	Porosity (%)	Brinell hardness (BHN)
AA2014-0	AA2014	2,800	2,720	2.86	79
AA2014-2	AA2014 + 2 vol.%	2,794	2,700	3.36	85
AA2014-3	AA2014 + 3 vol.%	2,791	2,667	4.44	89
AA2014-6	AA2014 + 6 vol.%	2,783	2,615	6.04	93
AA2014-9	AA2014 + 9 vol.%	2,774	2,598	6.34	99
AA2014-12	AA2014 + 12 vol.%	2,765	2,537	8.25	107

The graphs of theoretical and experimental densities and porosities of the composites according to the volume fractions of  $\text{B}_4\text{C}$  particles are shown in Figs. 4 and 5, respectively. Figure 4 shows that the theoretical density values of the composites decrease linearly (as expected from the rule of mixtures). Although a linear decrease was

also seen in the experimental densities, the values are lower than those of the theoretical ones. The density measurements showed that composites contain some porosity, and the amount of porosity in the composites increased with the increasing volume fraction of the particles (Fig. 5), as observed in the previous investigations [44–51].

The Brinell hardness of the composites and matrix alloy was given in Table 2. The relation between the particle volume fraction and the hardness of the composites is plotted in Fig. 6. It was seen from Fig. 6 that the hardness of the composites increased with increasing particle volume fraction. As compared to the 2014 Al matrix alloy, the hardness of the MMCs was found to be greater, and addition of  $\text{B}_4\text{C}$  particles increase the hardness of the Al alloy [45, 52].

Typical microstructures of the  $\text{B}_4\text{C}/2014$  Al alloy composites are shown in Fig. 7. The most important factor in the fabrication of MMCs is the uniform dispersion of the reinforcements. Such distribution of  $\text{B}_4\text{C}$  particles was only achieved under the optimum process conditions given in the previous study [42]. It can be seen that the most of  $\text{B}_4\text{C}$  particles were dispersed throughout the matrix (Fig. 7a–b), but there exist macro or microgas blows and shrinkage porosity near  $\text{B}_4\text{C}$  particles (Fig. 7c). Irrespective of attempts to optimise the fabrication parameters, these

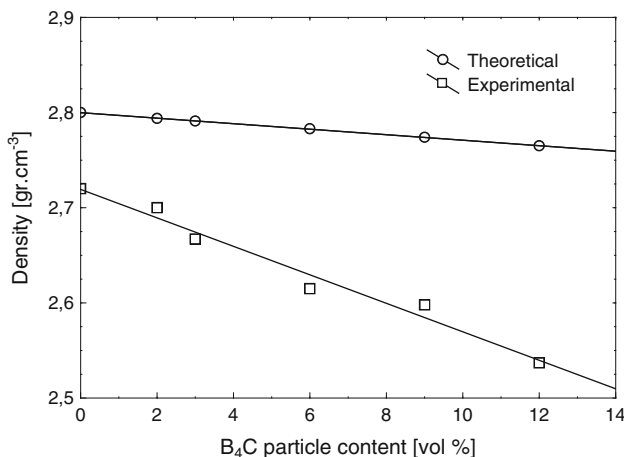


**Fig. 4** The variation of theoretical and experimental density with  $\text{B}_4\text{C}$  particle content

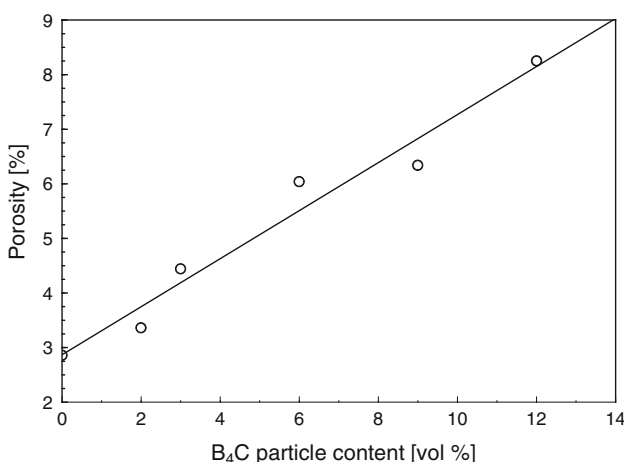


**Fig. 5** The variation of porosity with  $\text{B}_4\text{C}$  particle content

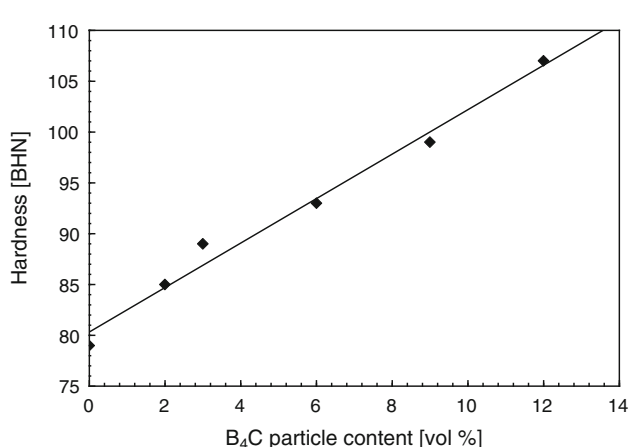


**Fig. 6** The variation of hardness with  $\text{B}_4\text{C}$  particle content

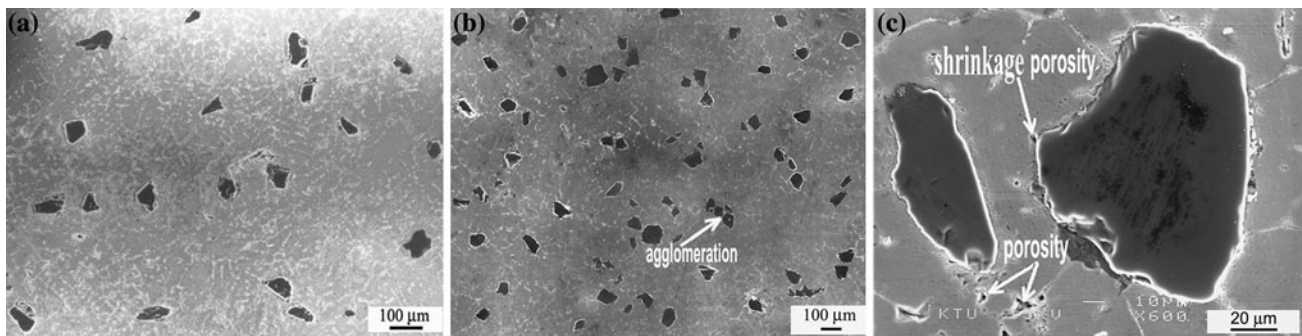


**Fig. 7** Microstructural characteristics of 2014 Al-B<sub>4</sub>C composites. **a** AA2014-3, **b** AA2014-9, **c** interface between B<sub>4</sub>C particle and matrix

defects are very difficult to overcome except using vacuum stirring techniques such as the Duralcan process [53]. Reasonably, uniform distribution of B<sub>4</sub>C particles in the AA 2014 matrix can be seen in Fig. 7a–b. The small-scale clustering of the reinforcing phase and agglomeration were clearly shown in Fig. 7b. Such phenomenon was also observed in different types of particles containing composites [54]. At typical higher magnification micrograph of composites clearly indicated a good interface bonding between B<sub>4</sub>C particle and the metallic matrix (Fig. 7c). No reaction product and no interfacial decohesion between the matrix and the B<sub>4</sub>C particles was found in the previous study [42].

The variations in volume loss with sliding time for unreinforced stircasting AA2014 alloy as well as for Al/B<sub>4</sub>C composites containing different volume percentages of B<sub>4</sub>C particles are summarized in Fig. 8. This figure shows the effect of sliding time on the average wear volume loss of the composites. It can be clearly seen from the figure that the volume loss increases with increasing sliding time and with decreasing particle content of B<sub>4</sub>C. The volume loss of the unreinforced alloy was found to be

much higher than that of the composites and it almost increased linearly with the sliding time. It can be observed that the composites show lower volume loss indicating the beneficial effect of the addition of B<sub>4</sub>C particles. This contribution may be attributed to the hardness of the material which is a dominating factor affecting the wear resistance. The decrease in wear volume loss may also be attributed to higher load bearing capacity of hard reinforcing material [55], which is similar to the observations obtained in some previous studies [56, 57].

The specific wear rates of the matrix alloy and composite containing B<sub>4</sub>C particles are plotted as a function of sliding time in Fig. 9. Generally, the specific wear rate decreased with sliding time and attained steady-state value. The wear behaviour of the samples was tested using an abrasive suspension mixture at room conditions. It was observed that the specific wear rate decreased rapidly during the initial stage and then decreased gradually with sliding time in the case of monolithic alloy. The composite showed superior wear resistance (inverse of specific wear rate) to that of the matrix alloy. Some researchers [58–60] mentioned that the wear rate of composites decreased

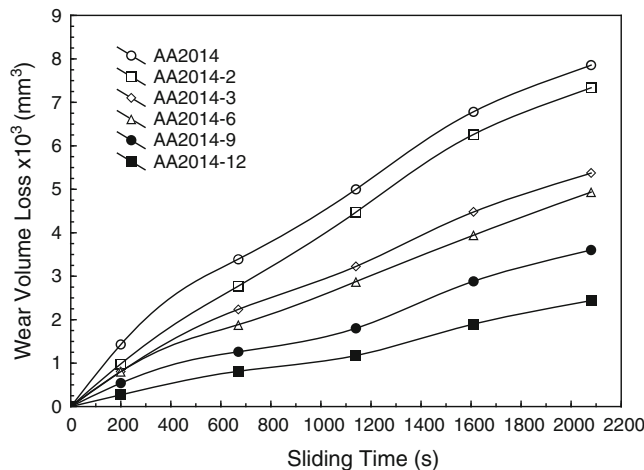


**Fig. 8** Variation of volume loss with sliding time at 92 N load for B<sub>4</sub>C particle reinforced composite

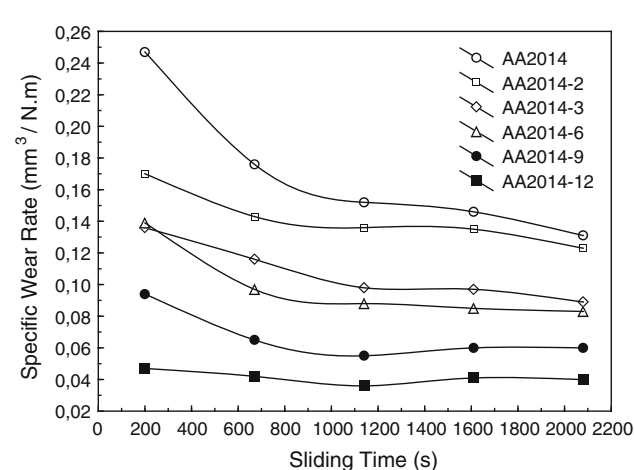


**Fig. 9** Specific wear rate of the matrix and the composite at 92 N load against the abrasive suspension

considerably with increasing reinforcement volume fraction. At the same time, the specific wear rate of composites decreased with increasing reinforcement volume fraction as seen in Fig. 9.

The hardness and roughness of the worn surfaces of Al alloy and composites were given in Table 2 and in Fig. 10, respectively. It is seen from these values that the surface roughness parameters ( $R_a$ ) decreased with increasing particle volume fraction in Fig. 10 whereas the hardness values increased with increasing particle volume fraction in Fig. 6. This means that, the higher the volume fraction of  $B_4C$  particles added to the aluminium alloy matrix, the better the wear resistance of the composites, similar to the observations of Lee et al. [61] and Yilmaz and Bultoz [62]. As a result, the abrasive suspension mixture is becoming more ineffective with sliding times because of the resistance offered by the hard dispersoid  $B_4C$  particles in the composite. This leads to faster and greater decrease in the surface roughness with increasing volume fraction in the composites as compared to the alloy. The abrasive wear of

a material depends on the elastic and plastic contact of the abrasives with the sample surface. During abrasive wear, the abrasive particles penetrate first into the specimen surface and then move over the surface due to reciprocating motion. Thus, continuous grooves are generated and these abrasive wear of a material primarily depends on the extent of the depth and width of the wear grooves and the number of grooves made by the abrasives. This is again dependent on the relative hardness of the abrasives with respect to the hardness of the sample. The composite exhibits almost 36% higher hardness than the alloy and hence the depth and width of the wear grooves are reduced significantly. Additionally, the hard ceramic dispersoid acts as a protrusion over the matrix and carries a major portion of the applied load. Such dispersoid particles protect the abrasives from penetration into the specimen surface [34, 63]. As a consequence, the depth and width of cut and the number of wear grooves produced in the composite surface are expected to be lower. It was observed that surface roughness increased rapidly with sliding time up to 200 s and then slowly increased or virtually standed with the sliding time for all samples after 200 s (Fig. 10).

Scanning electron micrographs of the worn surfaces of the composites and the matrix alloy are given in Figs. 11, 12, respectively. Mainly three body rolling wear that is characterized by multiple indentations and very short ploughing or cutting grooves was reported [64, 65]. The worn surface of the unreinforced 2014 Al matrix alloy was characterized by extensive plastic deformation and obvious evidence of ploughing, cutting and smearing (Fig. 11a–b). Since the unreinforced matrix alloy was much softer than the slider, the slider penetrated and cut deeply into the surface, causing extensive plastic deformation of the surface (Fig. 11a–b), and resulting in a great amount of material loss. For the composites investigated, the most important feature is the presence of  $B_4C$  particles having hardness value that is much greater than the matrix alloy. The  $B_4C$  particles in the matrix alloy protect the softer

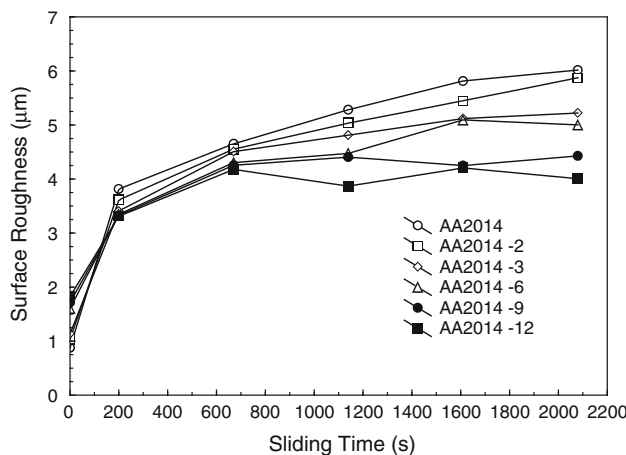


**Fig. 10** Variation of surface roughness of test samples with sliding time (normal load, 92 N; sliding speed, 0.314 m.s<sup>-1</sup>)

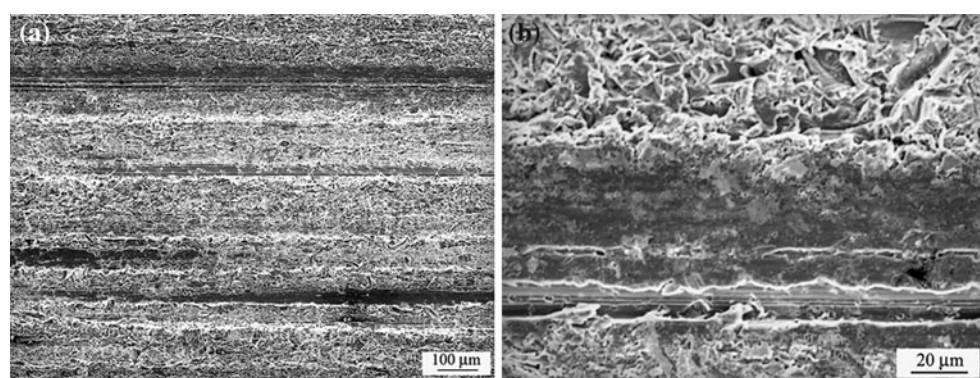


**Fig. 11** Wear surface of the matrix alloy (AA2014) tested at the applied load of 92 N over a sliding time of 2080 s **a** low and **b** high magnification

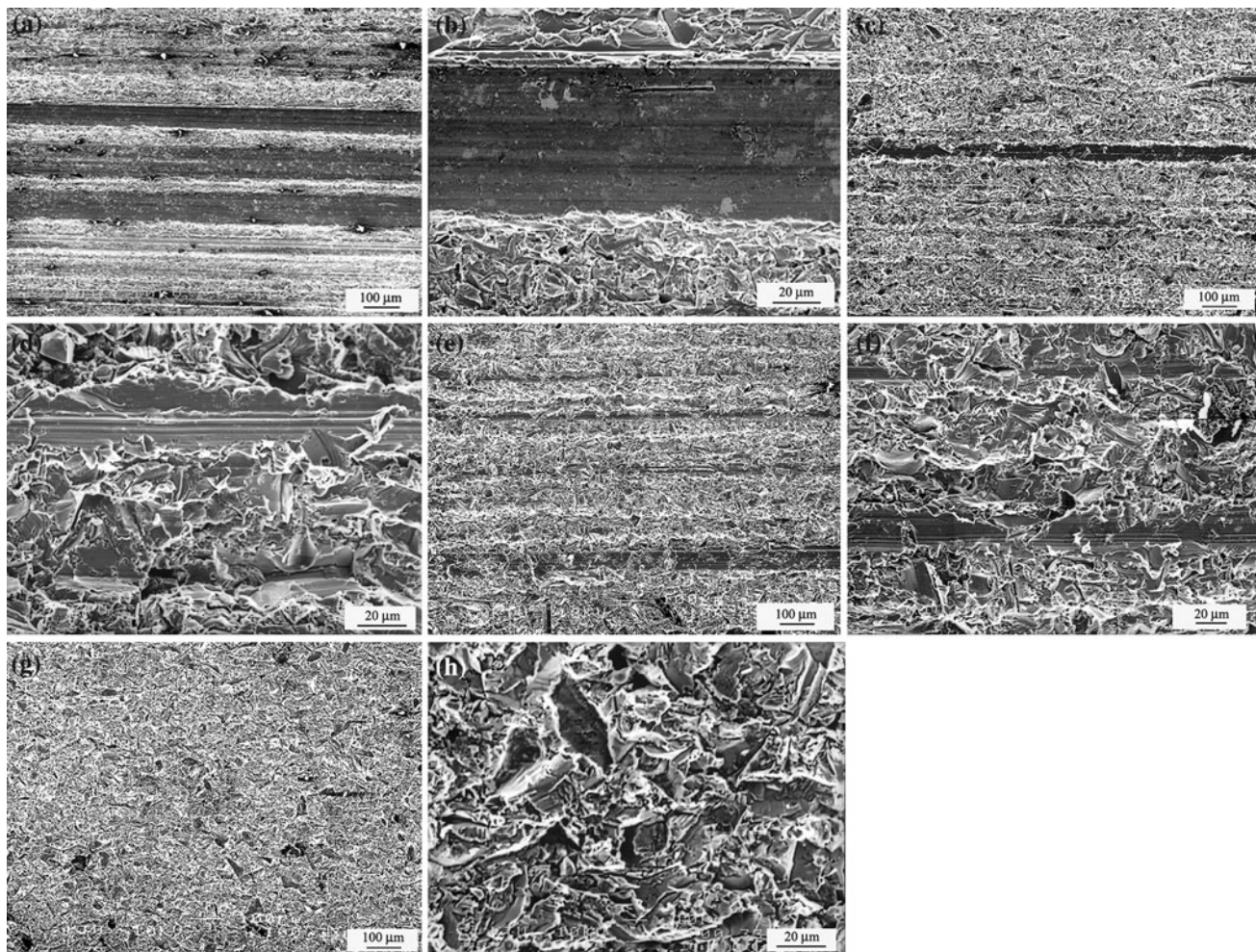


**Fig. 12** Wear surface of the composite tested at the applied load of 92 N over a sliding time of 2080 s **a** AA2014-3 (low magnification), **b** AA2014-3 (high magnification), **c** AA2014-6 (low magnification),

**d** AA2014-6 (high magnification), **e** AA2014-9 (low), **f** AA2014-9 (high magnification), **g** AA2014-12 (low magnification), **h** AA2014-12 (high magnification)

matrix during abrasive sliding and strengthen the aluminum matrix. These particles also resist the penetration and cutting of the slider into the surface of the composite, thus limiting the deformation. The wear resistance of the composites is therefore improved in comparison with the matrix alloy. The wear resistance of the particle reinforced composites are basically related to the wear resistance and hardness of the particles [66]. The worn surface of the sample AA2014-3 was somewhat analogous to that of the unreinforced matrix alloy, and was characterized by mainly plastic deformation with some ploughing and cutting effects (Fig. 12a–b). When the particle content was increased from 2 to 12 vol.%, the worn surface was characterized by localized grooves and fine scratches (Fig. 12a–h). On worn surface of the sample AA2014-9, the plastic deformation significantly reduced with increasing the  $B_4C$  particle volume fraction from 2% to 9%, and

the worn surface was characterized by localized shallow grooves and very fine scratches (Fig. 12e–f). Very little apparent plastic deformation was present on the worn surface of the sample AA2014-12 (Fig. 12g–h), and instead very fine scratches formed. Similar results have also been reported in some previous studies [46, 67].

## Conclusions

The following conclusions can be drawn from the present investigation:

1. Microstructural examination showed that the  $B_4C$  distributions were generally homogeneous in the AA2014 matrix while some particle clustering and the particle-porosity clustering were observed at

- relatively high particle containing composites. The density of the composite decreased with increasing particle volume fraction, but the porosity and hardness of the composite increased with increasing particle content.
2. The abrasive wear properties of the 2014 Al alloy were considerably improved by the addition of B<sub>4</sub>C particles, and the abrasive wear resistance of the composites was found to be much higher than that of the unreinforced 2014 aluminium alloy.
  3. The composite experienced lower materials loss than the matrix alloy under all test conditions employed. The wear volume loss of the matrix alloy and the composites slightly increased with increasing sliding time. However, the change of the wear volume loss for the composites with increasing particle volume fraction was smaller than that of the matrix alloy.
  4. The specific wear rate of samples swiftly decreased with increasing sliding time until a steady-state value of 670 s. Decreasing in the specific wear rate of samples above this value was very slow. Moreover, for composites containing the high amount of B<sub>4</sub>C particles, the specific wear rate of samples was found to be almost stable.
  5. Plastic deformation (micro cutting and micro ploughing) was identified as the main wear mechanism operating on the worn surfaces of the composites investigated. For the samples having by the addition of B<sub>4</sub>C particles, it was extensive plastic ploughing and cutting decreased. The depth and number of grooves in composites decreased with increasing volume fraction of B<sub>4</sub>C particles, and the worn surfaces of composites were relatively smooth.
  6. The surface roughness of the samples increased rapidly with sliding times up to 200 s and then increased slowly or virtually stood firm with the sliding time for all samples after 200 s. The surface roughness of the composites decreased generally with increasing the volume fraction of particles.

## References

1. Hunt M (1991) Mater Eng 108(6):27
2. Noguchi M, Fukizawa K (1993) Adv Mater Process 143(6):20
3. Yoshimura HN, Goncalves M, Goldenstein H (1997) In: Fuentes M, Martínez-Esnaola JM, Daniel AM (eds) Key engineering materials, vol 127–131(985–992). Transtech Publication Inc, Switzerland
4. Buhl H (1992) Advanced aerospace materials. Springer, Berlin
5. Weeton JW, Peters DM, Thomas KL (1987) In: Weeton J (ed) Engineer's guide to composite materials. ASM International, Metals Park, OH
6. Lloyd DJ (1994) Int Mater Rev 39(1):1
7. Prasad SV, Rohatgi PK (1987) J Metall 39(11):22
8. Pan YM, Fine ME, Chang HS (1990) In: Rothagi PK, Ian PJB, Yune CS (eds) Wear mechanism of aluminium based metal matrix composite under rolling and sliding contraction in technology of composite materials. ASM International, Metals Park, OH, p 93
9. Harris SJ (1990) Developments in particulate and short fibre composites in new light alloys. AGARD Lecture Series 144, p 1
10. Christman T, Needleman A, Suresh S (1989) Acta Metall 37:3029
11. Rohatgi PK, Asthana R, Das S (1986) Int Metal Rev 31(3):115
12. Rohatgi P (1991) JOM 43:10
13. Koczak MJ, Khatri SC, Allison JE, Bader MG (1993) In: Suresh S, Mortensen A, Needleman A (eds) Fundamentals of metal matrix composites. Butterworth-Heinemann, London, p 297
14. Howes MAH (1986) JOM 38:28
15. Ray S, Rohatgi PK (1972) Indian Patent No. 12430A
16. Badia F, Rohatgi PK (1969) Trans Am Foundrymen's Soc 79:402
17. Flemings MC, Mehrabian R (1976) New trends in materials processing. ASM International, Metals Park, OH, p 98
18. Ghosh PK, Ray S, Rohatgi PK (1984) Trans Jpn Inst Met 25:440
19. Suresh S, Mortensen A (1997) Int Mater Rev 42(3):85
20. Schicker S, Garcia DE, Bruhn J, Janssen R, Claussen N (1998) Acta Metall Mater 46(7):2485
21. Bhanuprasad VV, Staley MA, Ramakrishnan P, Mahajan PYR (1995) In: Newaz GM, Neber-Aeschbacher H, Wohlbier FH (eds) Key engineering materials, vol 104–107. Transtech Publication Inc, Switzerland, 495 pp
22. Stephens JJ, Lucas JP, Hoskins FM (1988) Scripta Metall 22:1307
23. Bonnen JJ, Allison JE, Jones JE (1991) Metall Trans 22A:1007
24. Prasad BK, Das S, Jha AK, Modi OP, Dasgupta R, Yegneswaran AH (1997) Composites A 28A:301
25. Sin H, Saka N, Suh NP (1976) Wear 55:163
26. Rabinowicz E, Mutis A (1965) Wear 8:381
27. Axen N, Zum Gahr KH (1992) Wear 157:189
28. Wang A, Rack HJ (1991) Wear 146:337
29. Moore MA, Douthwaite RM (1976) Metall Trans 7A:1833
30. Badse LJ (1968) Wear 11:213
31. Hutchings IM (1987) Chem Eng Sci 42(40):869
32. Murray MJ, Mutton PJ, Watson JD (1982) J Lubr Technol Trans ASME Tribol 104:9
33. Hornbogen E (1975) Wear 33:251
34. Prasad BK, Jha AK, Modi OP, Das S, Yegneswaran AH (1995) Mater Trans 36(8):1048
35. Kulik T, Kosel TH, Xu V (1989) In: Ludema KC (ed) Proceedings of the international conference on wear of materials, vol 1. ASME, Denver, USA, p 23
36. Jain Main T, Ye Ying S, Hua Ji Z, Chingan Z, Zianwu K (1985) Tribol Int 18:101
37. Zum Gahr KH (1979) Met Prog 116:46
38. Moore MA, King FS (1979) In: Proceedings of the conference on wear of materials. ASME, New York, USA, p 275
39. Hutchings IM (1991) In: Proceedings of the conference on advanced materials and processes. University of Cambridge, UK, p 56
40. Zum Gahr KH (1978) Z Metallkde 69:312
41. Catalog (2000) In: Tetrabor® boron carbide grains and powder. Wacker Ceramics. Wacker-Chemie GmbH Kempten Plant, Kempten, p 1
42. Canakci A, Arslan F, Yasar I (2007) J Mater Sci 42:9536. doi: [10.1007/s10853-007-1896-z](https://doi.org/10.1007/s10853-007-1896-z)
43. Braza JF, Cheng HS, Fine ME (1989) Tribol Trans 32(4):439
44. Manumanth GS, Iron GA (1993) J Mater Sci 28:2459. doi: [10.1007/BFO1151680](https://doi.org/10.1007/BFO1151680)
45. Kök M (2005) J Mater Process Technol 161:381
46. Kök M (2006) Composites A 37:457

47. Ghost PK, Ray S (1988) AFS Trans 775–782:88
48. Akhlaghi F, Lajervardi A, Maghanaki HM (2004) J Mater Process Technol 155–156:1874
49. McCoy OW and Franklin EW (1988) In: Fishman SG, Dhingra AK (eds) Cast reinforced metal composites. Chicago, USA, p 77
50. Ray S (1988) In: Fishman SG, Dhingra AK (eds) Proceedings of the survey on fabrication methods of cast reinforced metal composites. ASM/TMS, p 77
51. Cöcen U, Önel K (1996) Mater Sci Eng A 221:187
52. Purazrang K, Abachi P, Kainer KU (1994) Composites A 25(4):296
53. Hashim J, Looney L, Hashmi MSJ (2001) J Mater Process Technol 119:324
54. Hashim J, Looney L, Hashmi MSJ (2002) J Mater Process Technol 123:251
55. Suresh KR, Niranjan HB, Jebaraj PM, Chowdiah MP (2003) Wear 255:638
56. Das S, Das S, Das K (2007) Compos Sci Technol 67:651
57. Banerji A, Prasad SV, Surappa MK, Rohatgi PK (1982) Wear 82:141
58. Acilar M, Gul F (2004) Mater Des 25:209
59. Axen N, Jacobson S (1994) Wear 178:1
60. Axen N, Alahelisten A, Jacobson S (1994) Wear 73:95
61. Lee H-L, Lu W-H, Chan SL-I (1992) Wear 159:223
62. Yilmaz O, Bultoz S (2001) Compos Sci Technol 61:2381
63. Kulick T, Kosel TH, Xu Y (1989) In: Ludema KC(ed) Effect of depth of cut of two phase alloys. Proc Ins Conf Wear Mater, vol 1. ASME, New York, p 23
64. Rutherford KL, Hutchings IM (1996) Surf Coat Technol 79:231
65. Rutherford KL, Hutchings IM (1997) J Test Eval 25:250
66. Roy M, Venkataraman B, Bhanuprasad VV, Mahajan YR, Sundararajan G (1992) Metall Trans A 23:2833
67. Kök M, Özdiń K (2007) J Mater Process Technol 183:301